

# TailGator: Design and Development of Autonomous Trash collecting Robot

Subrat Nayak<sup>1</sup>, Bryan Hood, Owen Allen, Cory Foskey, Ryan Stevens,  
Edward Kallal, Jeff Johnson, Erik Maclean, Dr. Eric M. Schwartz

Machine Intelligence Lab (MIL),  
University of Florida,  
325 MAE Building B, PO BOX 116300,  
Gainesville FL 32611

Phone: (352) 392-6605

<sup>1</sup>email: sn32594@ufl.edu

## ABSTRACT

The autonomous robot discussed here was designed and built for the 2009 IEEE SoutheastCon Hardware Competition. The objective for the robot was to locate, pick up, sort and store beverage containers of different shape, size and weight as quickly as possible. The robot was required to operate inside a designated region bounded by a current carrying wire hidden beneath the field. The ground surface was covered with green AstroTurf. The beverage containers were Coca-Cola products (0.5-liter plastic bottles with caps, 8-ounce glass bottles and 12-ounce aluminum cans) lying flat on the ground in random orientations. A well designed robust system was needed to solve the problem. Necessary components in our solution included a pickup mechanism, a sorting mechanism, multiple smart sensors and an intelligent control algorithm.

## Keywords

TailGator, Grabber, Pet fence, Compass, Navigation, SoutheastCon, Autonomous, Robot

## 1. INTRODUCTION

Athletic stadiums and college campuses are plagued by the issue of trash after tailgating parties, after which there is often an assortment of glass, plastic, and aluminum beverage containers. This is unsightly, the clean up is time consuming, and represents a potentially significant source of untapped recyclable materials. By developing an autonomous robot that can locate, sort, and separately store the different containers, the manpower needed for cleaning can be significantly reduced. With this vision, the autonomous trash collecting robot being described in this paper was designed. The robot was the University of Florida's entry at the 2009 IEEE SoutheastCon Hardware Competition [1]. Dozens of possible solutions were considered and many experiments were performed in order to find a solution system comprised of a picking mechanism (that could retrieve containers placed in a wide range of orientations), a sorting mechanism (that was not significantly affected by environment conditions, vibrations or deformation in the containers), simultaneous management of Input-Output devices on an FPGA, and multiple smart sensors (including pet fence sensors, an electronic compass, small cone angle sonars, limit switches, current monitoring sensors and an intelligent control algorithm).

## 2. MECHANICAL DESIGN

The mechanical design of TailGator robot was significantly more challenging than any of the other IEEE hardware competitions in at least the last 7 years. The biggest challenges were to pick up

different sized objects that might be lying in random orientations and to make sure the whole robot could fit into a 12x12x18 inch box. Several weeks of brainstorming gave rise to a variety of designs for the picking and sorting mechanisms. Some designs were discussed that would not robot to stop to collect the recyclables. Some designs used rack and pinion systems while others used belts; some tried to bring the objects perpendicularly into the body of the robot, while others needed a two-axis robot arm.

Several gripper designs were considered. The chosen gripper was a compromise that ensured efficiency, reliability, met size constraints and was simple enough to be easily fabricated using inexpensive components and available machine shop equipments.

### 2.1 Platform Design

The platform (Figure 1) consists of the base, mounts for the gripper mechanism and drive system. The base was constructed of 1/2-inch thick acrylic sheet.

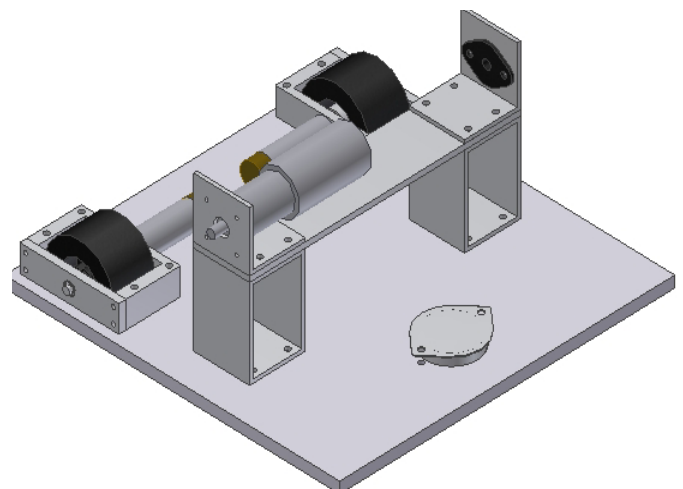


Figure 1: CAD of the PLATFORM

The drive system consists of a ball transfer unit (Figure 2) at the front and two motor drive systems. Since the ground was covered with AstroTurf, any wheel castor or normal ball castor would get stuck and/or restrict smooth Omni-directional motion. Hence, a ball transfer was chosen which consists of a single large steel ball resting on a number of small ball bearings encased in a steel cup with mounting flanges.



**Figure 2: Ball Transfer Unit– Top and Bottom View**

Each motor drive system (Figure 3) consists of a motor, wheel, hub, ball bearing and mounting bracket. The motor used is a permanent magnet 12V DC geared motor. These motors were chosen because their speed and torque characteristics were best suited for our application. The extended shaft on the rear of the motor allowed for the installation of encoders.



**Figure 3: DC geared motor**

Thick Foam wheels were chosen to achieve better traction on the Astroturf and to help in reducing the low frequency vibrations that occurred whenever the robot traversed over wrinkles in the Astroturf. Hub and mounting brackets (Figure 4) were machined out of aluminum stock. The other side of the hub shaft is press fit into a ball bearing which is again press fit into a hole on the side bracket. This design increases the load carrying capacity of the system.

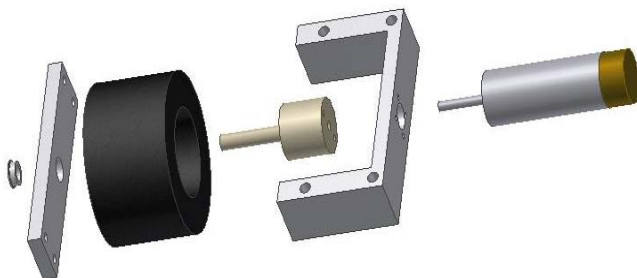


**Figure 4: Exploded view of drive system**

Assembling the drive motor systems is done by attaching the motor to the main mounting bracket. The hub is then attached to the motor shaft by using the set screws and aligning it with the motor shaft flat. The wheel is then screwed onto the hub. The side bracket is then attached to the main bracket, and the ball bearing is press fit into the side bracket and the hub shaft. Figure 5 shows an assembled drive system. Thin sheet metal guards (not

shown) were then put on the wheels to avoid any thing on the robot touching the wheels.

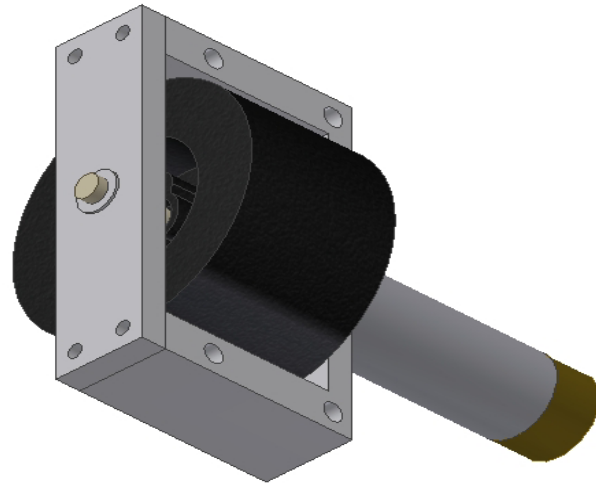


**Figure 5: Assembled view of drive system**

The gripper arm mount is made of two stands, an aluminum plate, two aluminum angle brackets, a pin bearing and a strong high torque low speed arm motor. The base also has two hard stops for the gripper arms. These are made up of 10-24 threaded rods with lock nuts.

## 2.2 Gripper Mechanism

The gripper mechanism shown in Figure 6 was used for picking up the containers. This mechanism is comprised of two gripper arms, atop gripper jaw and a bottom gripper jaw. These subassemblies are capable of moving independently to perform the motions required to pick up objects and move them to the sorter.

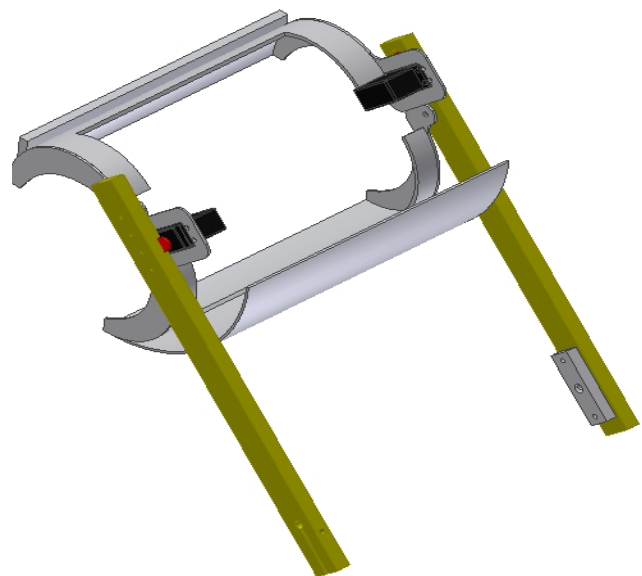


**Figure 6: Gripper mechanism for picking up objects**

The right gripper arm is attached to shaft of the motor on the gripper arm mount with an aluminum connector and a set screw. The left gripper arm is attached to the gripper mount using a pin

bearing and a small shaft. The right arm is actuated while the left arm, which is free to rotate, will follow the right arm to ensuring mechanical support without the cost of another motor.

The upper gripper jaw (on the bottom in Figure 6) is cut from a 5-inch diameter plastic tube. The lower gripper jaw (on the top in figure 6) is shaped from aluminum sheet metal. The jaws are then attached to the gripper arms using custom cut aluminum panels with servo housings and RC servos. When the servo motor rotates the jaw moves relative to the gripper arm. The bottom jaw is more complex in design; it has a distinctive bend in order to temporarily hold the container after being picked up and before being rolled down onto the sorting mechanism. This addition solved a previously observed problem where the container hit and became jammed against the servo body. With this addition, the container would roll back only when the gripper jaws were raised. This provided more time to ensure reliable identification with the sensor that was also housed in the crevasse that was created due to the bend.

This pick up mechanism proved to be both relatively simple and very efficient. The open jaws cover a large area on the ground to facilitate successful pick up of containers the different sizes shown in Figure 7. The sensors and navigation algorithm are expected to align the robot's front end parallel to the container to be picked, but neither the distance nor the orientation of the container with respect to the gripper could be assured. This simple gripper design generally compensated for even large errors in the distance and alignment to allow the robot to successfully pick up containers within a wide range of distances and orientations. If the container is not in the desired orientation, the gripper contributes to turning the container into the proper orientation when the gripper jaws start closing before picking it up.

The extreme case of container's long end lying approximately perpendicular to the front end of the robot should never happens due to the navigation sensors. If were to occur, the gripper jaws could get stuck, which will greatly increase the current. If a large current is detected with the current sensors, the control algorithm commands the gripper to release the container and to repeat the navigation and pick up process.

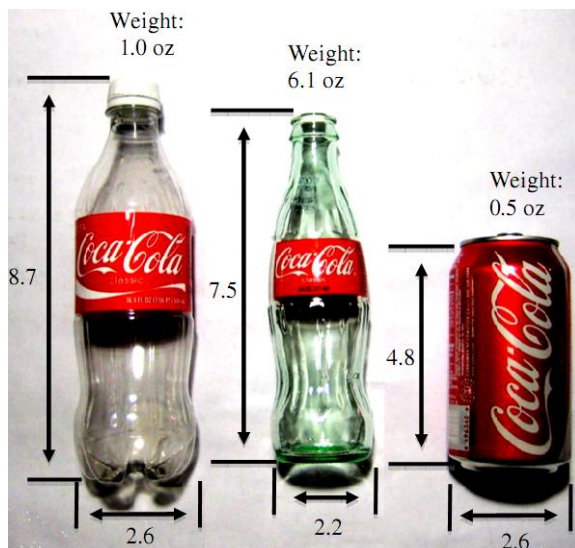


Figure 7: Beverage containers to be picked up

Two limit switches (of the type shown in Figure 8) were used at the two extreme positions of the arm. Open loop position control time limits were not adequate for protecting the motors. Hence, a closed loop positioning was achieved by installing limit switches at both extreme ends. As soon as the arm reaches a hard stop, a switch is triggered, which signals the processor to cut power to the motor.

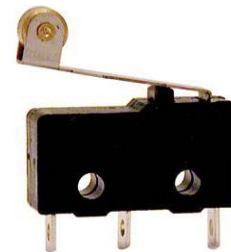


Figure 8: Micro switch

### 2.3 Sorting Mechanism

After the pickup and identification processes are done, the gripper rolls the container backwards along the sorter (Figure 9). The sorting mechanism consists of the aluminum stands, plastic frame held together by four angle brackets, collection bags and doors. The three doors completely cover the openings, are hinged on one side using simple loose nut-bolts, and opened/closed with a micro servo on the opposite end. The type of container determines which of the doors are opened and closed. The first door opens for glass bottles, the second door opens for plastic bottle (with the first door closed); therefore plastic bottles roll over the closed first door. The third door is always open so that when aluminum can is identified, the first two doors are closed and the can rolls into the open third door. The weights of each of the containers determined the ordering of the doors. The entire sorter frame is hinged onto the aluminum stands for rotational motion about a horizontal axis. In order for the entire robot to have a maximum starting size of 12"x12"x18", the sorter mechanism is folded vertically (the yellow bars in Figure 9 are rotate up approximately 90°. The sorter falls open (to the configuration in Figure 9) when the robot first moves. The position of the frame ensures a gradual slope so that the containers will roll after falling from the gripper jaws. The slope can be changed by two bolts that act as hard stops. This proved to be a very simple and flexible design. Collection bags are strapped onto the sorter frame using Velcro straps and can be removed when filled.

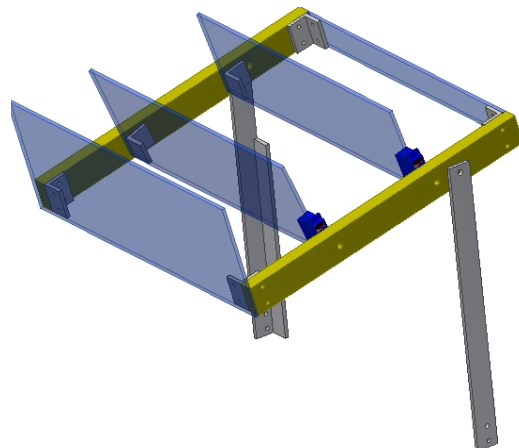


Figure 9: Sorter (Note the transparent doors)

To tackle worst case scenarios like the containers is still lying on the sorter and didn't roll into the right bag, the doors are opened and closed in front of the collection bag to push them into the correct bag. After the process is over the first two doors are closed. (The third door is always open.)

Because of the complexity of this project, AutoDesk Inventor was used to enable our mechanical development team to visualize and present the mechanical design and potential problems to the rest of the team for open discussions. All of the CAD figures in this paper were created with this software. Figure 10 shows the final CAD design for the robot.

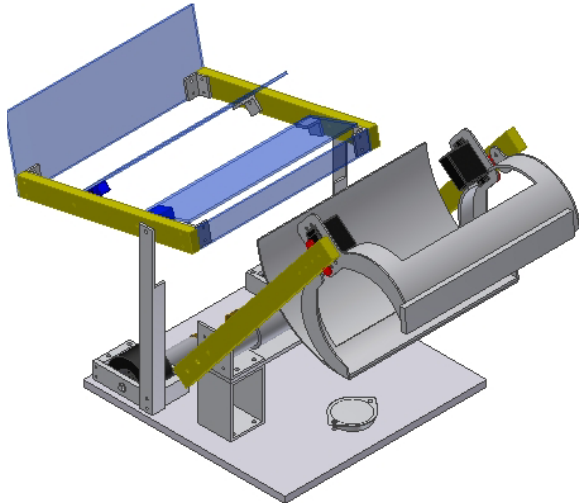


Figure 10: Fully Assembled Mechanical Hardware

### 3. ELECTRONIC HARDWARE

The electrical system consists of two batteries, two DC motors for driving the wheels, one DC motor for the gripper arm, two servos for the gripper jaws, two micro servos for the sorter doors, voltage regulators, two pet fence sensors, three sonars, a compass, a reflectance sensor array (identification sensor), five current sensors, three bidirectional motor drivers for the three DC motors, an LCD, an ATmega128 microcontroller board, and a Altera Cyclone II FPGA board.

#### 3.1 Power Supply

Two separate 14.8V LiPo 4450mAh battery packs are used. One is for all the actuators and the other is for the electronics. Lithium polymer batteries are preferable over other batteries because of their higher energy density and lower cell count. A steady 5V source is provided to all the electronics using a 5V, 1A switching voltage regulator (Figure 11). A steady 7V is provided to power the four servos using a 1A step down adjustable switching regulator (Figure 12). [2] [3]

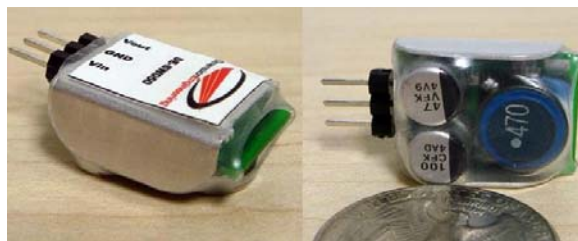


Figure 11: 5V, 1A switching voltage regulator

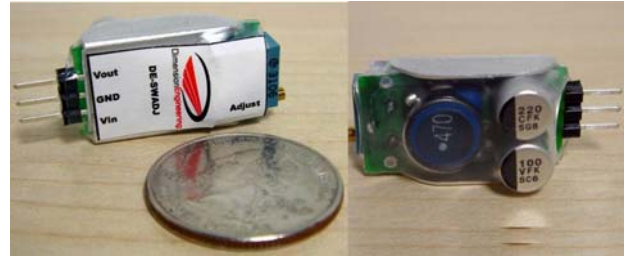


Figure 12: Adjustable switching voltage regulator

#### 3.2 SONAR

Three Devantech SRF05 sonars [4] (Figure 13) are installed on the front of the robot as distance sensors to locate the position of the container to be picked up. As per the rules of the 2009 IEEE SoutheastCon Hardware Competition, the beverage containers would never be closer than 12 inches from each other; hence, sonars were adequate to locate the containers.

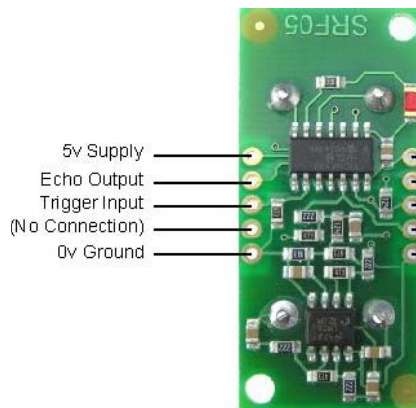
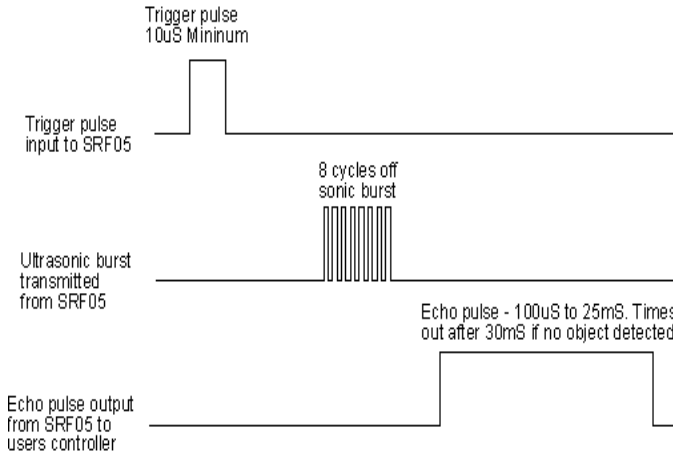


Figure 13: Devantech SRF05 SONAR

For this competition, knowing the distance of an obstacle (container) in front of the robot was not sufficient information; the robot needed to locate these containers. Once a container was located, the robot needed to move to an orientation that aligned the front edge of the robot approximately parallel to the longer edge of the container. To accomplish these tasks, three or more distance sensors with small cone detection angle were needed. Infrared (IR) based distance sensors were found to be less accurate than the sonars, and were also affected by the lighting conditions. The Devantech SRF08, Devantech SRF05 and MaxBotix EZ2 were all tested; the SRF05 was found to have the most narrow cone angle, the most accurate distance measurements, and were the easiest to interface to the microcontroller unit (MCU). We found that three of these sonars were adequate; three sonars provided enough information without having significant overlap of their detection cones.

The SRF05 has a transmitter and receiver tuned for 40kHz. The transmitter sends a 40kHz ultrasonic wave and the receiver

catches the reflected wave that bounces of an object. The distance is measured by converting the time it takes for the pulse to return. To communicate with the SRF05, the trigger pin (see Figure 13) needs to be pulled high for at least 10µs (Figure 14); this sends out the 40kHz ultrasonic wave. The echo pin remains high and changes to low when the reflected wave is received; if nothing is received by 30ms, then there is no object within range of the sonar.



**Figure 14: Interfacing the SRF05**

Since we were using three SRF05s, it was necessary to ensure that they were triggered at least 50ms apart so that the ultrasonic wave produced by one sonar would not be detected by the next sonar.

To ensure fast interfacing and to save MCU processing for high-level processing, the interfacing of the various sensors was done using an Altera Cyclone II FPGA. The FPGA logic was designed using Altera’s Quartus using VHDL. The VHDL code utilized one counter to hold the time taken for the signal to bounce back and three latches, which were triggered by each of the echo lines. When the echo returns, the current counter value was latched. The higher the time, the farther the object was from the sonar.

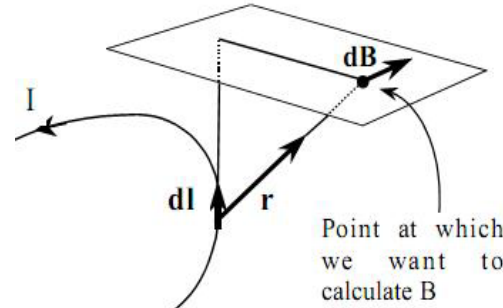
### 3.2 Pet Fence Sensor

The “pet fence” is an invisible fence or boundary placed around the perimeter of a home’s yard and is designed to contain the pets within the boundaries of the property. The pet fence normally carries a high frequency AC signal while the pet wears a light weight receiver collar which emits a warning sound when the pet nears the fence. If the warning is ignored and the pet approaches even closer to the fence, the collar gives a mild electric shock to the pet that increases in intensity as the pet moves closer to the fence. The pet soon learns to avoid the invisible fence location, making it an effective barrier. A pet fence was laid around the perimeter of the robot’s designated area of operation. The robot was supposed to remain inside this area during the entire competition run. Since the pet fence was custom designed to work at 10kHz and carry 25mA peak current, a ready made pet fence collar could not be modified with additional circuitry to give a signal to the MCU instead of the electric shock. The 10kHz and 25mA signal was too weak to directly detect since the signal induced on an antenna is directly proportional to the frequency and current.

Biot-Savart’s Law [5] describes the magnetic effect of current (Figure 15). The magnetic field at a point at distance  $r$ , due to a differential element of wire of length  $dL$ , and carrying current  $I$ , is given by

$$d\vec{B} = \frac{\mu_0\mu_r}{4\pi} \frac{I d\vec{L} \times \vec{r}}{r^3}, \quad \text{Equation 3.2.1}$$

where  $\mu_0$  is the permeability of free space/vacuum and  $\mu_r$  is the relative permeability of the medium.



*The symbols in boldface denote vector quantities.*

**Figure 15: Biot-Savart’s Law**

Therefore, the instantaneous magnetic field  $B$  (Figure 16) for a long straight wire, carrying current  $I$ , at distance  $D$  is given by

$$B = \frac{\mu_0\mu_r}{4\pi} \frac{2I}{D}. \quad \text{Equation 3.2.2}$$

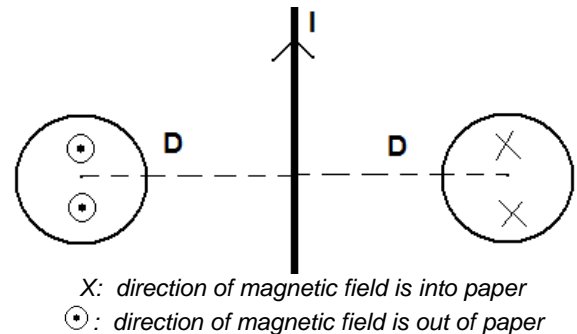


**Figure 16: Magnetic field due to a long current carrying conductor**

The pet fence was arranged to form a 10ft × 10ft square operating area. Figure 17 shows the contour plot of the magnetic field values at various points relative to a corner of the square operating region for a constant current flowing through the pet fence. The distance between the contour lines is not uniform and gets smaller for points nearer to the pet fence showing that the magnetic field is not uniformly distributed. Hence the field would be significantly stronger and detectable at points closer to the pet fence.

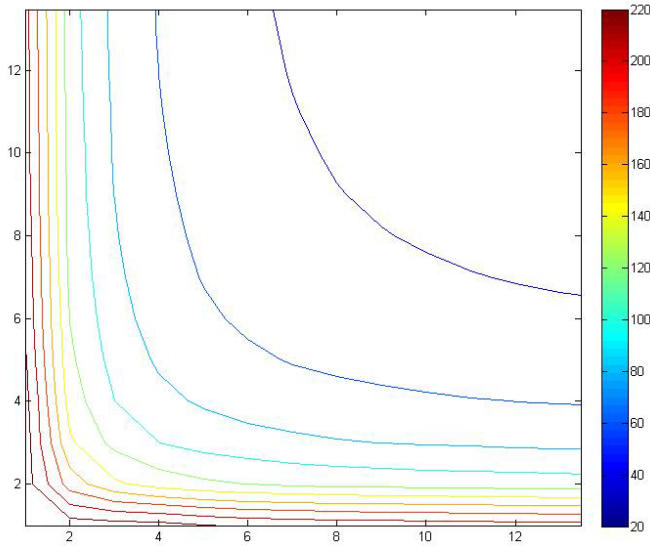


Figure 17: Contour plot of the magnetic field near a corner of the arena.

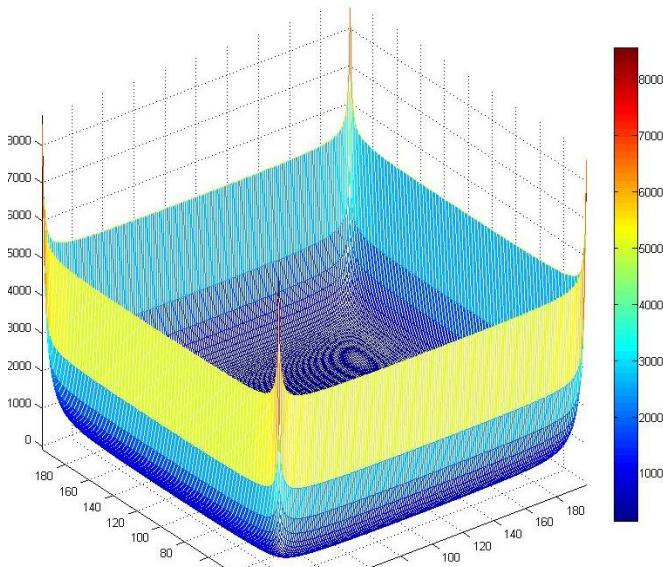


Figure 18: 3-D plot of the magnetic field values at various points throughout the operating region for a constant current flowing through the pet fence

From Eq 3.2.2, the flux linked with a coil placed at a distance  $D$  is given by

$$\Phi = BS = BnA = \frac{\mu_0\mu_r}{4\pi} \frac{2I}{D} nA \quad , \quad \text{Equation 3.2.3}$$

where  $n$  is number of coils and  $A$  is area of cross section. Hence, the emf ( $e$ ) induced in the coil is given by

$$e = \frac{d\Phi}{dt} = \frac{\mu_0\mu_r}{4\pi} \frac{2}{D} nA \frac{dI}{dt} \quad , \quad \text{Equation 3.2.4}$$

where only  $I$  is time varying quantity. For a sinusoidal current waveform,  $I = I_0 \sin(\omega t)$ , and therefore,

$$e = \frac{\mu_0\mu_r}{4\pi} \frac{2}{D} nA I_0 \omega \cos(\omega t) \quad \text{Equation 3.2.5}$$

We see that the emf induced in a coil is directly proportional to 1) frequency of the current, 2) amplitude of the current, 3) number of turns in the coil, 4) area of cross section of the coil, and 5) magnetic permeability of the core inside the coil. The emf is inversely proportional to the distance from the current carrying wire. Therefore, we decided to use a loop stick as the pet fence sensor. The setup works like an air core transformer. The pet fence acts as the primary winding and the sensor loop stick acts as the secondary winding which develops an induced emf whenever it is in the flux path. Since the frequency and current was fixed and low, the only way to significantly increase the signal strength of the induced emf was to make a loop stick with many of turns, a large area of cross section and to use a high permeability core material like ferrite rods. The loop stick also needed to be small and light enough to be fit on the robot. After much experimentation, a working loop stick was made from a plastic bobbin and thousands of turns of magnetic wire of small gauge. A compromise was achieved to ensure that the wire was thin enough to allow for a high number of turns, but strong enough so that it did not break during the winding process. The magnetic wire was wound over a bobbin using a small lathe machine and the core was filled with ferrite rings (as shown in Figures 19 and 20).



Figure 19: Ferrite ring used for core



Figure 20: Loop Stick

The loop stick is sensitive only to magnetic fields along its axis and hence needed to be mounted vertically as shown in Figure 20. Two of these were needed on the front edges of the robot in order to determine the direction of approach. The left loop stick would conceive a higher emf than the right loop stick if the pet fence is on the left side and vice versa.

In reality, the current waveform in the transmitter was not sinusoidal and contained all the odd harmonics of 10kHz. Hence, the induced emf on the loop stick also had the odd harmonics of 10kHz in addition to from the fundamental 10kHz signal. This was verified by viewing the Fourier transform of the induced signal on a Digital Storage Oscilloscope. There were many other undesired frequencies also present as noise in the induced signal. The 20kHz motor PWM, with current much higher than the pet fence sensor, was the major source of significantly strong noise. The 40kHz sonars were another source of noise. Since the loop stick is sensitive only to magnetic fields along its axis, any vibrations or movement of the loop stick also changed the induced voltage. This was another major source of low frequency noise, i.e., below 10 kHz. There was no power frequency noise because the robot was being powered with batteries. Radio signals also caused high frequency noise.

Hence, a band pass filter was needed to isolate and sense only the 10kHz signal. A very common approach used to pick up certain frequencies is to use parallel tuned LC circuits which resonate at

$$f_r = \frac{\omega}{2\pi} = \frac{1}{2\pi\sqrt{LC}} \quad \text{Equation 3.2.6}$$

But this needed accurate values of matched L and C values. Either the desired value of the L and C could not be found or the sizes of the components were too large. It also required constant tuning the circuit. One solution was to use a fixed capacitor and tune the inductor (the loop stick) by pushing a ferrite rod into the core or manually increasing or decreasing the number of turns on the loop stick. This process was very cumbersome and hence was abandoned. The simpler solution was to take the induced signal and pass it through a band-pass filter. A band-pass filter is a device that passes frequencies within a certain range and rejects (attenuates) frequencies outside that range.

An ideal band pass filter would have a completely flat passband (e.g., with no gain/attenuation throughout) and would completely attenuate all frequencies outside the passband. Additionally, the transition out of the passband would be instantaneous in frequency. In practice, no real band-pass filter is ideal. The filter does not attenuate all frequencies outside the desired frequency range completely; in particular, there is a region just outside the intended passband where frequencies are attenuated, but not rejected. This is known as the filter roll-off, and it is usually expressed in dB of attenuation per decade of frequency. Generally, the design of a filter seeks to make the roll-off as narrow as possible, thus allowing the filter to perform as close as possible to its intended design.

Two possible techniques for designing a steeper filter roll off are to increase the order of the filter and to increase the quality factor (Q) of the filter. Quality factor is defined as the center frequency of a filter divided by the bandwidth. The bandwidth is the frequency of the upper 3 dB roll-off point minus the frequency of the lower 3 dB roll-off point. The higher the Q, the better is the selectivity (see Figure 21); but with higher Q values, the filter becomes prone to instability. [6]

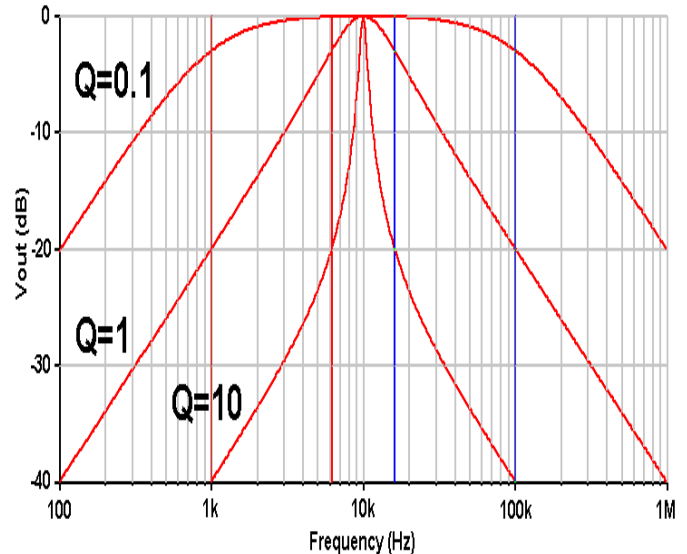


**Figure 21: Frequency response for different values of Quality Factor (Q)**

Band pass filters can be formed using multiple feedback op-amp circuits or using switched capacitor filters. The design of higher order band pass filters using op-amps were complex, required many extra components, and required non-standard resistor values. Use of dedicated switched capacitor filters seemed to be the simplest solution as they needed very few extra components, thus making the circuitry smaller and simpler. After rigorous searching and reading through data sheets of various switched capacitor filter ICs, the MAXIM MAX7490 (Figure 24) was chosen. This chip consists of two identical low-power, low-voltage, wide dynamic range, rail-to-rail 2<sup>nd</sup>-order switched-capacitor building blocks. Each of the two filter sections, together with two to four external resistors, can generate all standard 2<sup>nd</sup>-order functions: bandpass, lowpass, highpass, and notch (band reject) filters. Fourth-order filters can be obtained by cascading the two 2<sup>nd</sup>-order filter sections (as shown in Figure 24). The frequency response of a 4<sup>th</sup>-order filter like the one shown in Figure 24 is shown in Figure 25. Similarly, higher order filters can easily be created by cascading multiple MAX7490.

A switched capacitor circuit needs a clock signal for sampling. Since the clock-to-center frequency ratio is 100:1 in the MAX7490, a 1MHz oscillator was chosen to ensure a center frequency at 10kHz. Sampling is done at twice the clock frequency, further separating the centre frequency and Nyquist frequency. [7] [8] [9] [10]

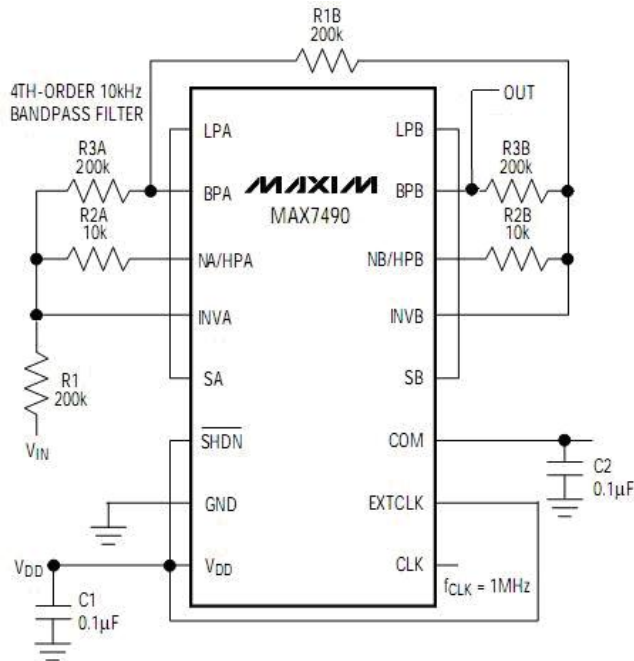


Figure 22: A 4<sup>th</sup>-order 10kHz band pass filter

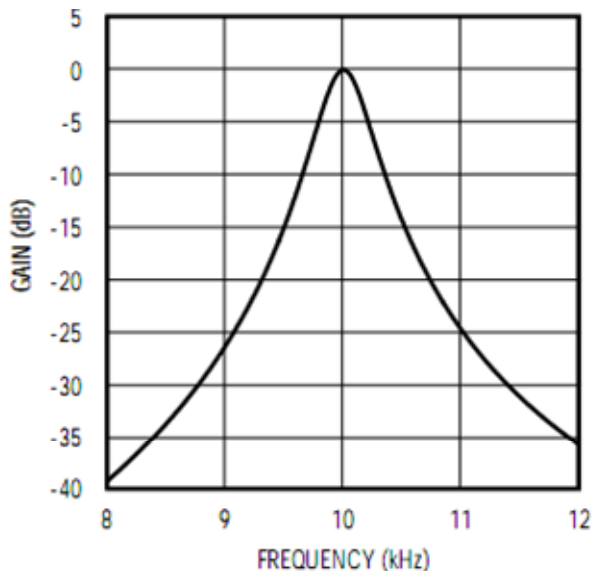


Figure 23: Frequency response of 4<sup>th</sup>-order 10kHz band pass filter using MAX7490

If the two loop stick sensors are placed on either side of the pet fence, the AC voltage induced on them will be 180° out of phase. This fact can be used to compare the phase of the AC signals on the two sensors and can be used to determine if the robot goes outside of the pet fence. The induced signal, even after filtering remains an AC signal whose amplitude represents the distance of the sensor from the pet fence. Hence, a peak detector circuit was needed to provide an analog DC voltage equal to the amplitude of the input AC signal. This was accomplished by using the op-amp circuit shown in figure 24. The DC analog voltage labeled PeakOut was input to the MCU’s analog-to-digital converter. [11]

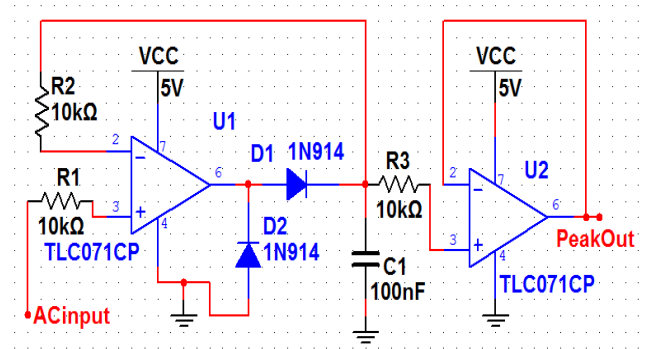


Figure 24: Peak detector circuit

### 3.2 Electronic Compass

To keep track of the robot’s relative orientation, the robot used a tilt compensated TCM2 electronic compass [12] (Figure 25) made by PNI Sensor Corporation. This sensor provides very accurate and noise free digital data in serial RS232 format and can be calibrated to compensate for soft and hard iron magnetic interferences. The orientation data, along with the pet fence sensor data, helps in navigating in the designated area, allowing the robot to efficiently explore the entire region. When the robot senses the pet fence (i.e., the current carrying wire), the compass provides the information necessary to turn the robot 90° towards the designated area. Without the compass data, the robot may end up following the pet fence and never explore the inner regions of the designated area.

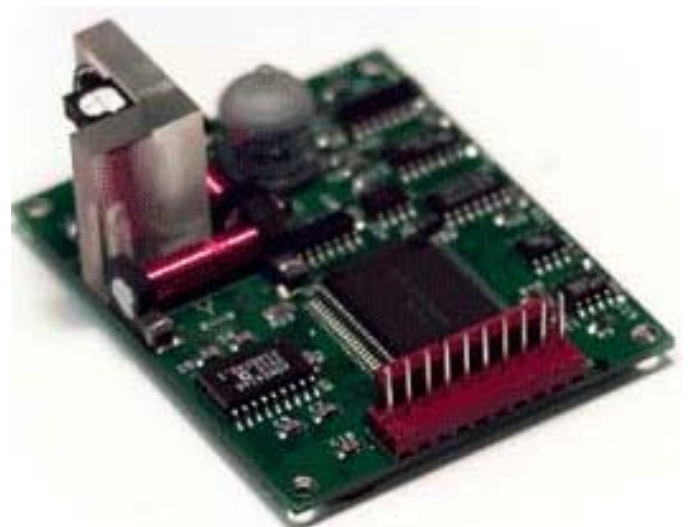


Figure 25: TCM2 Electronic Compass

### 3.3 Reflectance sensor Array

One of the challenges was to differentiate between aluminum cans, plastic bottles, and glass bottles. Overcoming this challenge meant finding a property that distinguishes all three containers. We chose to focus on the physical properties that can be easily detected.

Several alternatives were considered including weight, light absorption, and length. Since all the containers vary in length, it is possible to sort the containers with different-sized openings. In this design, the containers would pass over three openings of

different size while rolling down a ramp. Only the smallest object (can) would fall in the first opening, only the glass bottle would fit in the second opening, and the plastic bottle would be the only container remaining for the last opening. However, all the containers are tapered. This means it is possible for the tapered end of a glass or plastic bottle to jam into the smallest opening. Hence, this design was abandoned.

Differentiating the containers based on weight requires extremely precise sensors to accurately measure the small difference among their weights (especially between the can and the plastic bottle). This approach was not cost effective.

Another approach we tried was to use an infrared LED and a phototransistor to measure the amounts of light that passed each object. This approach was not mechanically feasible since we found that both the LED and the photo transistor needed to touch opposite sides of the object for successful identification. However, this approach was incorporated in our final solution which utilizes reflectance sensors to measure the length of the opaque (mostly red-colored) labels (see Figure 7) on each of the Coca-Cola (Coke) containers.

After a container is picked up, it falls into a crevasse inside the gripper jaws where the container lies aligned with an array of twenty reflectance sensors. The reflectance sensors measure the length of the red coke label by determining the number of sensors that return values below a threshold. A low value indicates an opaque object is in front of that sensor. The number of sensors that detect an opaque object determine the identity of the container..

The QTR-1RC reflectance sensors [13] (Figure 26), purchased from [www.pololu.com](http://www.pololu.com), were used. Each sensor consists of an infrared LED, a phototransistor, a 10nF capacitor and two resistors (150Ω and 220Ω). The schematic is shown in Figure 27.

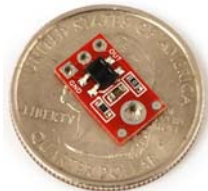


Figure 26: QTR-1RC reflectance sensor (on a quarter).

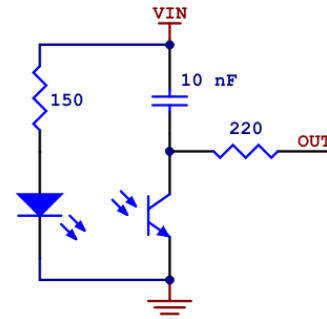


Figure 27: QTR-1RC reflectance sensor schematic

The coke label reflects the IR light, thus reducing the resistance of the phototransistor. The approach uses a bidirectional digital I/O line that first charges the capacitor by making the output pin (OUT) high for 10μs and then measuring the time for the capacitor to discharge through the phototransistor. Shorter discharge time implies higher reflectance or lesser resistance between the OUT pin and ground. The discharge time is compared to a predefined threshold value which is chosen so that only the reflectance of the opaque label is considered reflectance. This approach ensures higher sensitivity and lesser noise compared to voltage-divider type resistance measuring circuits which give analog voltage outputs.

The simultaneous reading of all 20 sensors is ensured by using VHDL-defined components created on an Altera Cyclone II FPGA. This facilitates quick and efficient sensing while allowing the MCU to be used solely for high-level decision making rather than interfacing with slow sensors. The length of the (mostly red) opaque coke labels are measured by the number of the consecutive sensors that sensed reflectance. The FPGA outputs the result to the MCU through a 2-bit digital value (as shown in Table 3.3.1). Figure 28 shows the PCB design of the reflectance sensor array.

Table 3.3.1: Reflection sensor FPGA-uP interface

Output	Interpretation
00	No object
01	Can
10	Glass bottle
11	Plastic bottle

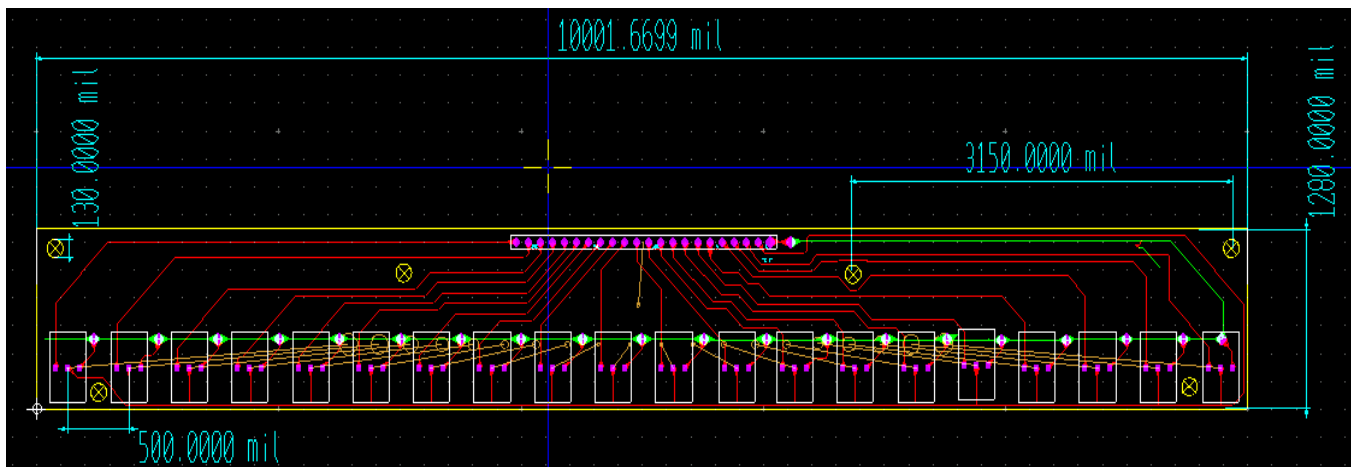


Figure 28: Reflection Sensor PCB Design

### 3.4 DC Motor Driver

The DC motors were driven in both directions using Freescale MC33887 motor driver H-bridge ICs (Figure 29). These drivers are capable of running DC motors at 5-28V and drawing up to 2.5A. The speed of the motor is determined by PWM signals provided to the motor driver. The duty cycle (on-time) of the PWM signal is proportional to the speed. The direction is chosen by two direction pins on the motor driver (as shown in Table 3.4.1).

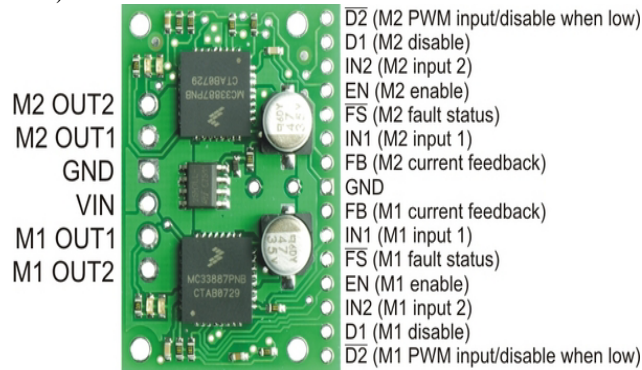


Figure 29: Dual MC33887 Motor Driver Board

Table 3.4.1: Truth Table for Direction lines

Input	Function
00	Stop
01	ACW
10	CW
11	Never -

### 3.5 UF4712 Cyclone II FPGA board

An FPGA was chosen to offload data acquisition and motor control from the microcontroller and thus allowing the MCU to focus solely on the decision making and high level algorithms. The UF-4712 FPGA board [14] (Figure 30) was selected. (This board, designed by UF students, is used in UF’s Digital Design course, EEL4712.) The UF-4712 board consists of a Altera Cyclone II EP2C8T144C8 FPGA, two dual-digit 7-segment displays, a ten LED bank, two 8-pin dip switch banks, and four momentary push buttons. It also has USB connector, VGA connector, PS/2 connector, and a JTAG programming header for the Altera Byte Blaster.

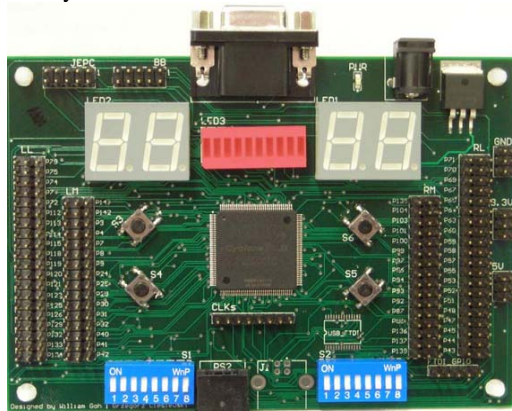


Figure 30: UF-4712 Cyclone II FPGA board

A parallel interface to the MCU was chosen for simplicity. The bus consisted of eight data lines, four address lines, a read/write signal and an enable. Internal to the FPGA, there were two buses; one was used entirely for motor control and the other for the sensors. Each sensor element went through a tristate buffer, which was combined with the motor control bus at a bidirectional buffer to the microcontroller. Each sensor element consisted of a process block which interpreted data from various sensors and then placed the data into a one byte register. This register could be accessed by the MCU at any time. The motor control elements consisted of a register and a PWM generator. The registers stored data so that each PWM kept a desired value (proportional to the duty cycle) until the registers were over written by a new desired value.

### 3.6 ATmega128 Microcontroller

The main decision making and high level algorithm were run on an 8-bit Atmel Atmega128 microcontroller [15] running at 16MHz. The BDMICRO Mavric IIB board [16] (Figure 31) was selected for this purpose. ATmega128 has 128K program flash, 4K static RAM, 4K EEPROM, two 8-bit timers, two 16-bit timers, 8-channel 10-bit ADC, analog comparator, dual USARTs, SPI, and I2C interfaces. The board also provides on-board level shifters to offer true RS232 and RS485 voltages and has both JTAG and ISP programming headers.

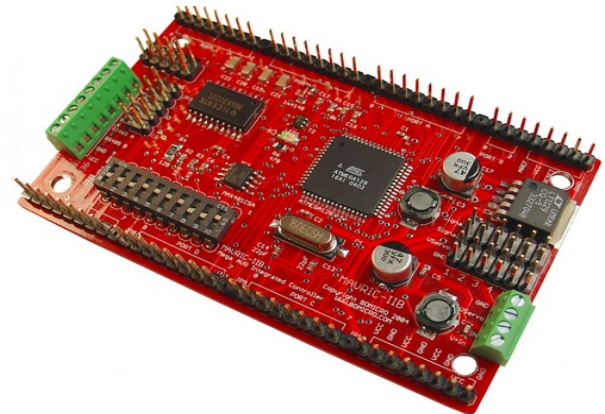


Figure 31: Maveric IIB ATmega128 board

## 4. FUNCTIONING OF THE ROBOT

### 4.1 Initial start up

In the initial start up position of the robot, the gripper arms are raised, and the sorter is raised to a near vertical position, giving the robot initial starting dimensions of approximately 12”x12”x18”. In order to operate, the sorter must be lowered to its functional position. This is accomplished by the robot quickly accelerating forward for a short distance, and then lowering and raising the gripper arms. If the initial forward motion of the robot does not cause the sorter to drop, the raising of the gripper arms will push the sorter over into its functional position.

### 4.2 Drive

The robot is driven by applying power to the drive motors. Providing equal power to both motors results in the robot moving relatively straight. Turning is accomplished by varying the power given to each drive motor. Increasing the power to the right motor (or decreasing power to the left motor) results in a left turn. The front ball caster can freely roll in any direction. It functions only as third support and a means of stabilizing the robot. Using

this drive system, the robot is able to drive forward, reverse, and turn left and right.

### 4.3 Picking up Containers

In order to pick up an object, the robot keeps moving forward until the sonars detect the presence of some container within their ranges. Then, using the values of the three sonars, the robot moves towards the container, trying to align with it such that its in front of the robot (i.e., the central sonar can detect it, the distance of the container from the front is within a specified range, and the longer edge of the container is approximately parallel to the front edge of the robot). The gripper arms are then lowered with the jaws wide open. When the arms have fully lowered, the right arm triggers the limit switch that tells the gripper arm motor to stop. Both arms come to rest on the hard stops. The jaws are then closed, capturing the container. Due to the shape of the jaws and the containers, the captured container is forced into a parallel orientation within the jaws. In case the jaws get stuck or the container does not allow the arm to close, the current flowing into the gripper servos suddenly become very high; this is detected by the current sensors and the control logic commands the gripper to re-open. When the arm is raised to vertical and it has reached the extreme limit, another micro switch gets triggered that tells the gripper arm motor to stop.

### 4.4 Identification and Sorting

While the container is held inside the gripper jaws and the gripper arm is raised, the container falls into a crevasse where it gets aligned along the reflectance sensor array and is identified. Then, based on the type of the container, the appropriate door of the sorter mechanism is opened. The gripper jaws are then opened, causing the container to roll back and fall on the sorting mechanism and then rolling through the appropriate door into the awaiting bag. This raising motion is repeated three times to ensure that the object leaves the gripper. This repeated motion also helps push the object over the sorter in the event of an undesired exit from the gripper. As the gripper ramp is raised and lowered with the gripper, the ramp can push objects into better position to be collected.

Glass bottles will fall through the first door upon leaving the gripper ramp. Plastic bottles will roll over the first closed door (for glass) and fall into the second opening. Cans will roll over both the doors (for glass and plastic containers) and fall into the always opened third door (for cans).

Due to the possibility of an object not fully entering its proper collection bag, a preventative measure is taken. The doors in front of the active door is opened to help push the container into the next door opening. In the case of a collected can, the glass door is raised and lowered, followed by the raising and lowering of the plastics door. This motion acts to move any object that did not fully roll over the sorter down towards its collection bag; it will also help to move any object that did not fully enter its bag to complete its journey into it the proper bag and off of the sorter.

Once the above sequence is completed, the both of the two container doors are closed. The robot then resumes its search for additional objects. The maximum amount of objects the robot can collect is five cans, three plastic bottles, and two glass bottles.

### 4.4 Navigation

The primary navigation sensor of the robot is the sonar. The robot locates and aligns with containers using the sonars. The next

important navigation sensor is the pet fence sensor. If any pet fence is detected and the left pet fence sensor has a greater value than the right sensor, the pet fence is on the left side of the robot and hence the robot takes a sharp 90° right turn. The robot uses the compass to achieve the 90° turn. This navigation algorithm helps the robot to increase the areas of exploration and discovery than it could achieve with a blind search. Without a compass, the turn angle cannot be guaranteed, which may cause the robot to continue moving along the fence and never actually moving towards the central regions of the operating area.

Since the sonars cannot see the containers from long distances, the robot keeps moving forward expecting to encounter a container or the pet fence. This could have been avoided and the whole process accomplish more efficiently by using a camera that could see from far away and guide the robot. Experiments were performed with a USB camera that would capture 320x240 pixel sized pictures of the field and look for the color red. Each object had a significant portion of red on its label that was easily distinguished from a green background with our image processing algorithms. In order to reduce the effects from lighting, the images in RGB space images were converted to HSV space. Simply looking at the hue values in the image and applying a double threshold to isolate the red hue, a binary image was produced that contained only the red labels. Then, using contour finding algorithms, the individual objects were located. The container lying lowest on the image was the nearest to the robot and was the first target. All the image processing was done using the OpenCV computer vision processing library [17] on an embedded computer board that was supposed to be housed on the robot. The embedded computer was to communicate with the micro controller board via serial RS232 protocol. But due to complexity of the system, and the success of the sonar system, the use of the camera was discarded.

## 5. ACKNOWLEDGMENTS

We would like to thank IEEE Atlanta Section and Georgia Tech IEEE student branch for hosting the 2009 IEEE SoutheastCon Hardware Competition, which motivated us to work hard for this project. We are also grateful to the Machine intelligence Laboratory (MIL) at UF, where all of the research, design, testing, and most of the construction occurred. We wish to thank the IEEE Gainesville section and Gainesville section student branch at UF for providing us the funds to turn our ideas into a functioning robot. We express our special gratitude to our faculty advisors for all their support, encouragement and advice. We are also thankful to STMicroelectronics, Maxim, Texas Instruments and Linear Technologies for providing free samples of various ICs. Finally, we are indebted to other members of the MIL and the teaching assistants of EEL4924C (Senior Design) and EEL5666C (Intelligent Machines Design Laboratory) courses who helped us with advices, resources and encouragement.

## 6. REFERENCES

- [1] "IEEE SoutheastCon2009 Hardware competition Rules and Transmitter," August 2008.
- [2] Dimension Engineering DE-SWADJ Adjustable Switching Voltage Regulator data sheet, <http://www.dimensionengineering.com/DE-SWADJ.htm>

- [3] Dimension Engineering DE-SW050 5v Switching Regulator data sheet, <http://www.dimensionengineering.com/DE-SW050.htm>
- [4] "SRF05 - Ultra-Sonic Ranger Technical Specification," <http://www.robot-electronics.co.uk/html/srf05tech.htm>
- [5] David J. Griffiths, *Introduction to Electrodynamics (3rd Edition)*, Prentice-Hall, London, 1999.
- [6] MAXIM application note 733: "A Filter Primer," [http://www.maxim-ic.com/appnotes.cfm/an\\_pk/733/](http://www.maxim-ic.com/appnotes.cfm/an_pk/733/) October 2008.
- [7] Bruce Carter, "A Single-Supply Op-Amp Circuit Collection" (Texas Instruments), <http://www.ti.com/litv/pdf/sloa058> November 2000.
- [8] Ron Mancini, "Op Amps for Everyone" (Texas Instruments), <http://focus.ti.com/lit/an/slod006b/slod006b.pdf> 2002.
- [9] "MAXIM MAX7490 Dual Universal Switched-Capacitor Filters," [http://www.maxim-ic.com/quick\\_view2.cfm/qv\\_pk/2325](http://www.maxim-ic.com/quick_view2.cfm/qv_pk/2325) 2007.
- [10] MAXIM application note 3494: "The Basics of Anti-Aliasing: Using Switched-Capacitor Filters," [http://www.maxim-ic.com/appnotes.cfm/an\\_pk/3494/](http://www.maxim-ic.com/appnotes.cfm/an_pk/3494/) April 2005.
- [11] Ramakant Gayakwad, *Op-Amps and Linear Integrated circuits (4th edition)*, Prentice Hall, London, August 1999.
- [12] "TCM2 Electronic Compass Module User's Manual" (PNI Sensor Corporation), [http://www.pnicorp.com/files/TCM2.5\\_31-March-2009.pdf](http://www.pnicorp.com/files/TCM2.5_31-March-2009.pdf) April 2002.
- [13] "Pololu QTR Reflectance Sensor Application Note," [http://www.pololu.com/docs/pdf/0J13/QTR\\_application\\_note.pdf](http://www.pololu.com/docs/pdf/0J13/QTR_application_note.pdf) 2009.
- [14] Eric M. Schwartz, et al., "UF-4712 Board Manual" Revision 1.7, [http://www.mil.ufl.edu/4712/docs/uf-4712\\_board/UF-4712\\_Board\\_Manual\\_v1.7.pdf](http://www.mil.ufl.edu/4712/docs/uf-4712_board/UF-4712_Board_Manual_v1.7.pdf), from UF's EEL4712: Digital Design, September 2008.
- [15] "Atmel ATmega128: 8-bit AVR Microcontroller with 128K Bytes In-System Programmable Flash," [www.atmel.com/atmel/acrobat/doc2467.pdf](http://www.atmel.com/atmel/acrobat/doc2467.pdf) June 2008.
- [16] "BDMICRO MAVRIC-IIB ATmega128 AVR Integrated Controller II Technical Manual" Revision B, <http://www.bdmicro.com/mavric-iib/mavric-iib.pdf>, March 2009.
- [17] Gary Bradski and Adrian Kaehler, *Learning OpenCV: Computer Vision with the OpenCV Library*, O'Reilly, September 2008.

## 7. ROBOT PICTURES

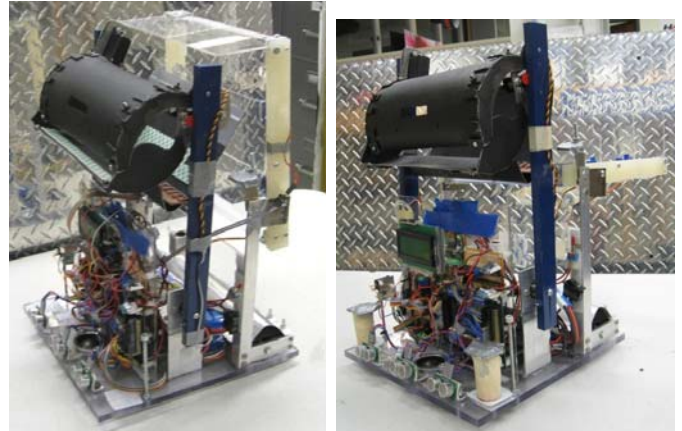


Figure 31: TailGator in home position (left) and with sorting mechanism deployed (right)

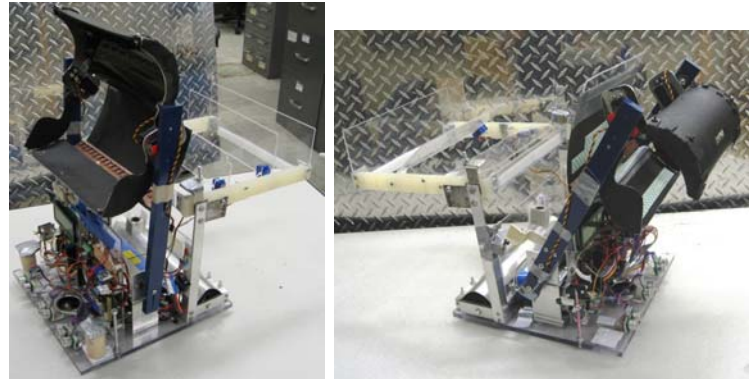


Figure 32: TailGator with grabber fully open (left) and partially open (right)



Figure 33: TailGator in container retrieval position